ZSM-5 surface modification by plasma for catalytic activity improvement in the gas phase methanol-to-dimethylether reaction

Josefine Schnee, Maxwell Quezada, Oriana Norosoa, Federico Azzolina-Jury

Version of Record: https://www.sciencedirect.com/science/article/pii/S0920586119301269
Manuscript_4758a13c6e288ee9c33df774f15b5927

ZSM-5 surface modification by plasma for catalytic activity improvement in the gas phase methanol-to-dimethylether reaction

Josefine SCHNEE~~Oriana NOROSOA~~[1], Maxwell QUEZADA[1,2], Oriana NOROSOA~~Josefine SCHNEE~~[1], Federico AZZOLINA-JURY[1]*

[1] Normandie Université, ENSICAEN, UNICAEN, CNRS, Laboratoire Catalyse et Spectrochimie, 14000 Caen, France

[2] Normandie Univ, UNIROUEN, INSA Rouen, LSPC, Laboratoire de Sécurité des Procédés Chimiques 76000 Rouen, France

*Corresponding author. E-mail address: federico.azzolina-jury@ensicaen.fr

Abstract

Dimethylether (DME) is nowadays considered as one of the most promising alternative fuels for the future. It has a very low climate impact~~, as it burns without emission of soot or SO_x, and with extremely reduced emission of NO_x, CO and CO_2. It~~, and can be produced in a renewable way, namely from the gas phase condensation of methanol ~~(available from biomass)~~ over common acid catalysts such as γ-Al_2O_3 or zeolites. The challenge today is to switch from high reaction temperatures (300-350°C) to lower ones (ideally 100-150°C) in order to operate ~~1)~~ more energy-efficiently and ~~2)~~ with 100% selectivity to DME~~, thus by avoiding the formation of coke which blocks the access to the acid sites and thereby deactivates the catalyst (an important issue with zeolites)~~. The methanol conversion needs to be increased below 300°C in order to get high yields of DME even in that low temperature range. In the present paper, we show a way to achieve this in the case of the widely studied ZSM-5 zeolite. We show that submitting the zeolite to a cold plasma treatment before using it as a catalyst ~~in the methanol-to-DME reaction~~ allows significantly increasing the yield of DME up to 300°C. Indeed, the plasma treatment ~~(monitored thanks to *operando* FTIR)~~ leads to a partial dealumination of the zeolite ~~(as shown by XRD and MAS ^{27}Al NMR),~~ and thereby to an increase of the number of strong Brønsted acid sites ~~(as evaluated thanks to *in situ* FTIR upon pyridine adsorption)~~ which play a key role in the methanol-to-DME reaction mechanism.

Keywords: Alternative fuels; Dimethylether; Methanol condensation; Plasma; Zeolites; Dealumination

1 Introduction

Dimethylether (DME) is nowadays of great interest in energy and environmental chemistry. It is called "the fuel for the 21st Century" by some research teams **[1]**. It can be used in diesel engines instead of conventional fuels, as hydrogen source in fuel cells, or as cooking gas instead of LPG (Liquefied Petroleum Gas) **[1-3]**. Actually, it should be considered as the fuel of choice for eliminating the dependency on petroleum **[4]**. As it has no C–C bond and contains no sulfur, DME burns with no emission of soot or SO_x. It also leads to extremely reduced NO_x, CO and CO_2 emissions **[4]**. Moreover, DME is non-toxic, non-corrosive and biodegradable **[2-5]** and it is qualified as clean alternative fuel **[1,4,6]**. Besides, DME can also be used as an intermediate for the synthesis of various important chemical compounds such as light olefins and aromatics, or it

could be also transformed into methyl acetate, formaldehyde and ethanol *via* reaction with CO or syngas **[3]**.

DME can be produced from the one-step conversion of syngas using a bifunctional catalyst (typically based on Zn and Cu supported on Al_2O_3), or from the gas phase condensation of methanol (the intermediate of the two-step conversion of syngas) over an acid catalyst **[3,7]**. In any case, as syngas can be produced from biomass, DME appears as a renewable fuel.

The gas phase condensation of methanol ($2\ CH_3OH \leftrightharpoons CH_3OCH_3 + H_2O$) is the most mature route and is therefore widely used in chemical industries **[3]**. It is generally performed at atmospheric pressure over common acid catalysts such as γ-Al_2O_3 or zeolites (ZSM-5, ZSM-22, Y, SAPO-34...), at reaction temperatures between 200 and 360°C **[3,6,8]**. γ-Al_2O_3 is reported to be highly selective to DME (near to 100%) up to a temperature of *ca.* 325°C, above which CO and CH_4 appear **[9]**. In contrast, over zeolites, generally leading to higher methanol conversions than γ-Al_2O_3 due to their higher acid strength, undesired by-products and coke (carbonaceous deposits hindering the access to the acid sites) are formed reducing the selectivity to DME and leading to catalyst deactivation **[6,8,10]**. Among the volatiles, typical by-products are alkanes (such as methane, propane, butane, pentane, heptane), olefins (such as ethylene and propylene), and aromatics (such as toluene and xylene) **[11]**. Actually, consecutively to the methanol-to-DME reaction, the methanol-to-hydrocarbons (MTH) process gets additionally activated, leading to a so-called "hydrocarbon pool" **[6,12]**.

In order to limit the MTH process, responsible for coke deposition, researchers are generally focused on the development of new catalyst design and/or on the modification of experimental conditions **[3,6,7]**. For example, supporting ZSM-5 on SiC foams was shown to lead to the formation of small zeolite crystals that favors the diffusion of DME throughout the porous network and thereby significantly reduces the consecutive formation of hydrocarbons **[13]**. However, the preparation of such catalysts is deemed quite complex **[6]** and 100% of selectivity to DME is not achieved. Performing the reaction under air was also tried. Indeed, over SAPO-34 and ZSM-5, the presence of air in the feed was shown to negatively impact the production of olefins at 350°C. Nevertheless, again, 100% of selectivity to DME was not achieved **[6,14]**. Actually, to really minimize the MTH process, the methanol reaction should be operated at lower temperature (typically 100-150°C) **[8]**, what would be also, by the way, more energy-efficient. A more efficient methanol production at low temperature can be performed using alternative catalysts with higher acid strength, such as heteropolyacids **[8,15,16]**, or finding new strategies to increase the acidity of the catalysts.

Zeolites are crystalline aluminosilicates with 3D regular structure. They are widely used in the industry and academic world **[17-25]**. Several studies have been addressed in order to increase zeolites catalytic activity. One interesting approach is based on zeolite partial dealumination for acidity modification. González et al. performed HCl acid treatment of several zeolites under microwave irradiation **[26]**. They observed an increase in surface area, mesoporosity and strength of Brønsted acid sites. Another interesting proposal is the zeolite acidity modification by acid leaching treatment using HF aqueous solutions **[27-29]**. After the acid treatment of zeolites, the number of strong Brønsted acid sites is decreased and the number of Lewis acid sites increased *via* partial dealumination of zeolites. Moreover, the concentration of HF acid solutions was found to play a crucial role on the strength of acid sites. Desilication of zeolites in an alkaline medium such as NaOH has also been proposed for the selective framework silicon etching **[30,31]**. Intercrystalline mesoporosity is observed after silicon leaching. The secondary mesoporosity usually involves aluminium redistribution towards the external surface of zeolite crystals increasing thus Lewis acidity without modifying Brønsted acidity **[30]**.

Besides, the desilication process shortens the micropores length, which is desirable for reactants diffusion, and also increases the number of available active acid sites at the pore months **[31]**.

The use of plasmas has gained attention during the last decades and it has been proven to be a very promising technology for the preparation of efficient catalysts. Liu et al. **[32,33]** reported, in a very interesting review, the use of cold and thermal plasmas in the preparation of materials. Plasmas could be used in the different steps of catalysts preparation or synthesis such as drying, decomposition, reduction, oxidation and regeneration **[33]**. Plasmas are also used for catalyst surface modification. Plasma surface modification treatment of materials has shown to improve catalytic activity of materials and to reduce their deactivation through the improvement of metal dispersion. Low temperature plasmas have been applied as well for zeolites activation including organic template removal and cold calcination of NH_4-zeolites **[34-36]**.

We have recently reported the use of cold plasma (low pressure glow-like discharge) for the novel preparation of alumina from boehmite with a remarkably improvement of final textural properties **[37]**. We have also recently reported basicity improvement of Ni(Mg,Al)O hydrotalcite-derived catalysts promoted by low pressure glow plasma discharge **[38]**. Liu et al. **[39,40]** reported catalytic activity and stability enhancement as well as Brønsted and Lewis acidities improvement of ZSM-5 catalysts after plasma treatment using a glow discharge.

In this work, we put in evidence the acidity improvement of organic-free template ZSM-5 zeolite by cold plasma activation using a glow-like discharge at low pressure. Indeed, we demonstrate that the plasma activation allows significantly increasing the ZSM-5 catalytic performance in the subsequent methanol-to-DME reaction, in particular at temperatures as low as 150°C as a consequence of zeolite acidity enhancement.

2 Experimental section

2.1 Organic template-free ZSM-5 synthesis

ZSM-5 organic template-free hydrothermal synthesis has been widely studied **[41-45]**. In this work, ZSM-5 without organic template was synthesized with a Si/Al molar ratio of 40 with the following molar gel composition: $100SiO_2$:$12Na_2O$:$5Al_2O_3$:$2500H_2O$. Ludox HS-40 colloidal silica was used as silica source (40% SiO_2 in water, Sigma Aldrich). Sodium aluminate (technical, anhydrous Sigma Aldrich) was used as aluminum source. Sodium hydroxide (BDH Prolabo VWR Chemicals; 98% purity) was adopted as alkali metal salt.

In a PFTE flask, 0.8 g of NaOH and 1.15 g of $AlNaO_2$ were dissolved in 43 mL of distilled water under continuous stirring. Afterwards, 23.25 mL of Ludox solution were slowly added. The homogeneous synthesis gel was aged during 24 h at room temperature and then introduced into a PFTE reactor of 100 mL. The synthesis mixture was then placed in an oven at 180°C for 48 h. At the end of the crystallization step, the reactor was cooled down to room temperature. The solid product was recovered by filtration and exhaustively washed with distilled water until reaching a pH of 7. Finally, the powder was dried in an oven at 120°C for 1 h. The final zeolite powder was weighed and a yield of 80% was obtained on the basis of SiO_2. After the synthesis, the Na-ZSM-5 form was obtained. In order to obtain the NH_4-ZSM-5 form, sodium ion was exchanged by ammonium ion *via* ion exchange at 80°C using a 1M solution of NH_4NO_3 in distilled water. The ion exchange process was carried out during 3 h and repeated three times. The zeolite powder was filtered and dried in an oven at 120°C for 1 h between the successive ion exchange steps. The final NH_4-ZSM-5 form was divided into two batches. The first one was

calcined under air at 400°C during 4 h with a heating/cooling rate of 3°C.min^{-1} in order to obtain the H-ZSM-5 form *via* thermal calcination. This zeolite will be named hereafter as H-ZSM-5 without plasma treatment. The second one was calcined using cold plasma at low temperature (near room temperature) using a glow-like discharge under partial vacuum (3 mbar) during 20 minutes. This zeolite will be named hereafter as H-ZSM-5 with plasma treatment. Before catalytic testing, the two zeolites were pre-treated/activated both in the same way inside the catalytic reactor, as described in section 2.4.

2.2 Zeolite activation by low temperature plasma

A plasma *operando* IR-cell detailed in a previous work **[23,24,37,38]** was used for cold calcination (plasma treatment) of NH_4-ZSM-5 zeolites. Zeolite powder was pressed (1.96.10^5 Pa) into self-supported wafers (2 cm^2, ~20 mg) for infrared (IR) measurements during plasma treatment. In this IR plasma cell, the wafer was located in down position in order to be irradiated by the glow-like discharge within the zone located between the two electrodes. The plasma discharge was generated using a high voltage AC power supply (Resinblock transformer FART, 50 mA) at 2 kV and 50 Hz. The gas system including mass flow controllers (Brooks) was connected to the top of the plasma IR cell. A molar mixture of 80% Ar and 20% O_2 was used for plasma treatment. The latter was followed by *operando* IR spectroscopy with a Bruker Vertex 80 v FTIR spectrometer between 4000 and 1000 cm^{-1} (1 cm^{-1} optical resolution) and an MCT detector.

2.3 ZSM-5 physico-chemical characterization

The ZSM-5 structure and crystallinity were verified after synthesis and after plasma treatment using a PANalytical X'Pert PRO diffractometer with CuKα radiation (λ = 0.15418 nm, 40 mA, 45 kV). The X-ray diffractrograms were acquired between 2θ = 5-60° at intervals of 0.1° with a scan speed of 2° per min.

Nitrogen adsorption-desorption isotherms were measured at 77 K with a Micrometrics Model ASAP 2020 volumetric adsorption analyzer. Zeolite samples were outgassed at 220°C overnight before analysis. The ZSM-5 specific surface area was determined from the Brunauer–Emmet–Teller (BET) equation and the average pore volume was estimated from the N_2 adsorbed volume at P/P^0 = 0.99.

Magic angle spinning ^{27}Al nuclear magnetic resonance (MAS ^{27}Al NMR) was used to investigate the ZSM-5 dealumination after plasma treatment. Analysis was carried out at room temperature on a Bruker Avance-500 spectrometer operating at 11.74 T (500 MHz), using a 4 mm zirconia rotor with a spinning rate of 14 kHz (radiofrequency of 107.1 kHz (ν_1^{Al}), recycle delay of 1 s, 512 scans). The chemical shift scale was calibrated with respect to a sample of liquid $Al(NO_3)_3$.

In situ Fourier-transform infrared (FT-IR) spectroscopy upon pyridine adsorption-desorption was used to quantify the total number of acid sites of ZSM-5 zeolite before and after plasma treatment ("total" means both outside and inside the pores, as pyridine is able to enter the pores). Samples were pressed into a self-supported disc (2 cm^2, ~20 mg). The resulting pellets were placed into a homemade IR cell equipped with KBr windows. Nicolet Nexus one equipped with a KBr beam splitter and DTGS detector was used. Spectra were recorded with a 4 cm^{-1} optical resolution. The samples were pre-treated for 4 hours under vacuum (until reaching 10^{-6} Torr) at 400°C before pyridine adsorption. A 3°C min^{-1} ramp was used to heat the pellets from

room temperature to 400°C. Afterwards, they were exposed to 1 Torr of pyridine, first at room temperature and then at 100°C, both times for 1 hour. Finally, during pyridine evacuation (until reaching 10^{-6} Torr), the samples were left at room temperature for 1 hour and then heated successively up to 100-150-200-250-300-350-400-450°C (by moving the pellet down to the IR beam and up again to the furnace in-between two successive temperatures), for 40 minutes at each temperature. FT-IR spectra were measured at room temperature during and/or after each step (always after in the case of heating steps because of the setup configuration).

Thermogravimetric analysis (TGA) was used to determine the amount of coke deposited on the samples at the end of the catalytic tests. It was performed on a thermogravimetric analyzer (PerkinElmer, Pyris 1) under a nitrogen flow of 80 mL.min^{-1} (STP). Samples of 5 mg samples were placed in ceramic pans and analyzed from 30 to 900°C with a heating rate of 20°C min^{-1}.

2.4 Methanol-to-DME catalytic tests

ZSM-5 zeolite powder (100 mg sieved within 150-300 µm) was introduced into a packed bed reactor and placed inside an oven. ZSM-5 zeolite powder with plasma treatment was obtained by grinding the wafers of 20 mg used during the FTIR *operando* study described in section 2.2. The experimental set-up was connected to a gas distribution system and to a gas chromatograph. First of all, the catalyst was activated for 4 hours under air at 400°C with a flow rate of 25mL.min^{-1} (STP). A 3°C min^{-1} ramp was used to heat from room temperature to 400°C. Before reaction, the catalyst was cooled down from 400 to 100°C. 25 mL.min^{-1} (STP) of nitrogen (Linde gas, 99.995%) saturated with 17 vol.% of methanol was introduced to the reactor (Acros Organics, 99+% extra pure) at atmospheric pressure. The reaction was performed from 100 to 450°C. The outlet gas flow was analyzed with a Varian CP 3900 gas chromatograph equipped with a WCOT CP-Wax 52 CB 2.0 µm column (35 m x 0.25 mm) and a FID detector. Analyses were performed 10 times for each temperature every 50°C from 100 to 450°C. A heating rate ramp of 3°C.min^{-1} was used for changing the reaction temperature. The reaction temperature was recorded using an 8 channels temperature data logger TC-08 of Pico Technology.

3 Results and discussions

3.1 ZSM-5 crystallinity and textural properties after plasma treatment

~~The XRD patterns of the ZSM-5 samples are shown in Figure 1. The initial crystallinity of ZSM-5 was not modified after all chemical and thermal treatments. However, a shift was observed at 7.9° of 2θ between the H-ZSM-5 with and without plasma treatment indicating a possible dealumination after plasma treatment.~~

The XRD patterns of the ZSM-5 samples are shown in Figure 1. The initial crystallinity of ZSM-5 was not modified after all chemical and thermal treatments. All samples presented characteristic XRD peaks of MFI structure at 2θ = 7.90°, 9.04°, 23.28°, 24.16° and 25.63°. Not any amorphous phases or other crystalline phases were observed, indicating that all zeolites, with and without ammonium and after treatment with and without plasma, were pure ZSM-5 crystals. However, a variation in the relative intensity of XRD peaks was evidenced indicating a relative crystallinity loss of ZSM-5 zeolite after plasma treatment. This loss of crystallinity by plasma treatment has already been reported in literature **[46]**. The decrease in XRD relative intensity of ZSM-5 characteristic peaks after plasma treatment could suggest some morphologic

changes in zeolite crystallites. The peak at 9.04°, ascribed to {200} facet, was increased and the one at 7.9° associated to {101} plane, decreased when plasma was used. This is probably due to a partial dealumination caused by plasma which is later discussed in this work. The plasma induced a morphologic change of zeolite crystallites by shortening their size along the c-axis and by increasing their size along the b-axis. This can present an influence on the mass transfer properties of zeolites (tortuosity) and on their catalytic activity. Moreover, a shift was observed at 7.9° of 2θ between the H-ZSM-5 with and without plasma treatment indicating a possible dealumination after plasma treatment.

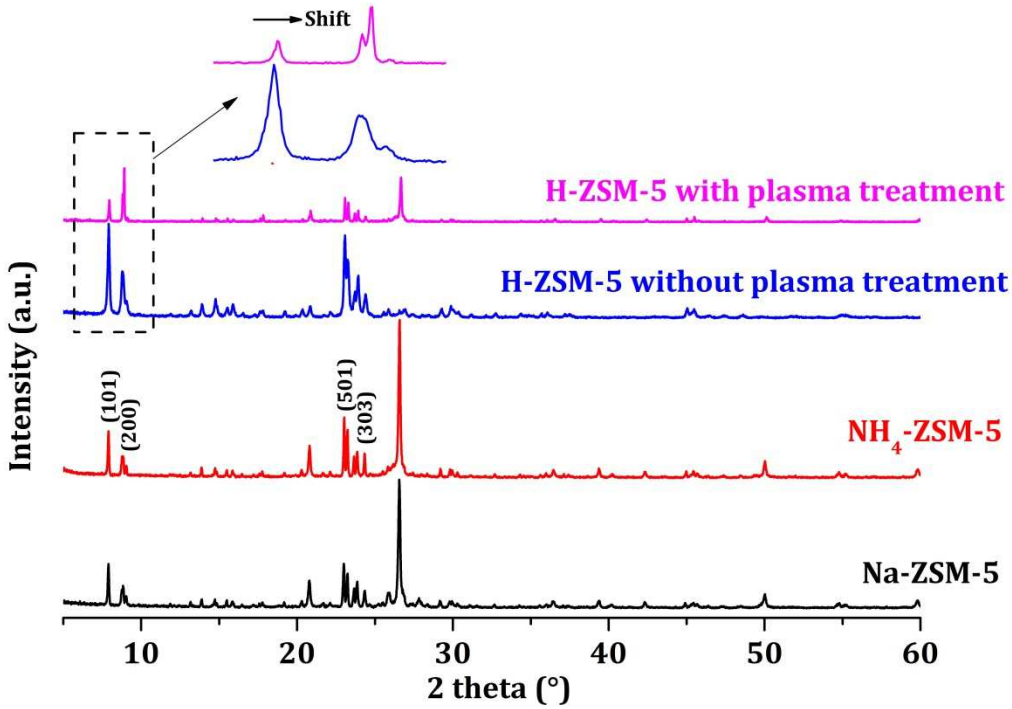

Figure 1: XRD patterns of ZSM-5 zeolites

The textural properties of H-ZSM-5 zeolites with and without plasma treatment are presented in Table 1.

Table 1: H-ZSM-5 zeolite textural properties with and without plasma treatment

H-ZSM-5	BET surface area ($m^2.g^{-1}$)	t-Plot micropore area ($m^2.g^{-1}$)	t-Plot external surface area ($m^2.g^{-1}$)	Pore volume ($cm^3.g^{-1}$)	BJH Pore size (nm)	Average particle size (nm)
Without plasma treatment	168.6	152.7	15.9	0.1	7.4	35.6
With plasma treatment	159.9	128.5	31.4	0.1	6.7	37.5

BET total surface area was decreased by 5% when plasma was used for obtaining the H-ZSM-5 form from the NH_4-ZSM-5 form. The micropore area was diminished by 15% and the external surface area improved by 49% when plasma was applied. This can be explained by the fact that plasma treatment is a surface treatment only since Debye length (µm), for this kind of plasma **[23,24,37,38]**, is 1000 orders of magnitude higher than the pore size (nm) and plasma cannot be formed inside the zeolite pores. Pore volume and sizes as well as particle size were not significantly different with and without plasma treatment.

3.2 Partial ZSM-5 dealumination and acidity improvement after plasma treatment

3.2.1 *Operando* FTIR cold plasma calcination of NH_4-ZSM-5 zeolites

The temporal evolution of NH_4-ZSM-5 IR bands followed by *operando* FTIR spectroscopy during cold plasma calcination is shown in Figure 2.

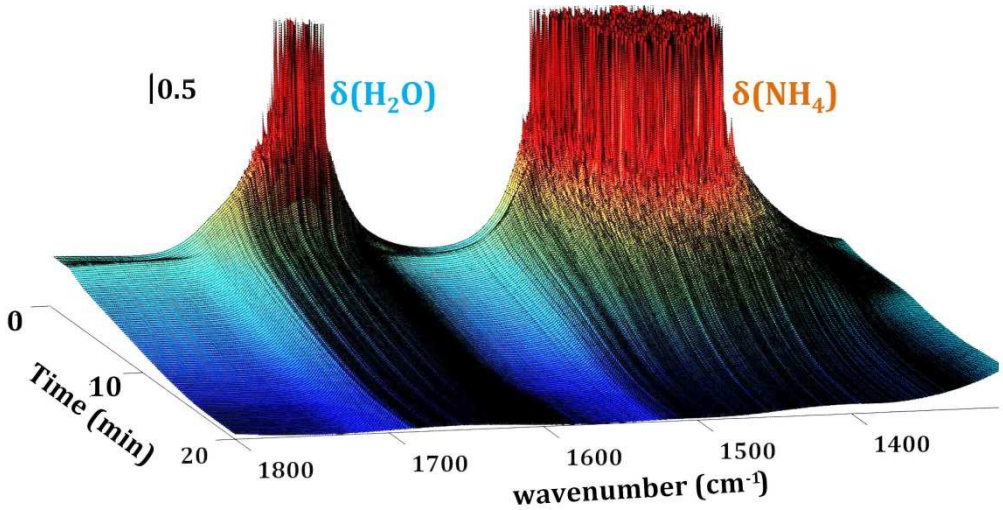

Figure 2: Temporal evolution of NH_4-ZSM-5 IR bands during cold plasma calcination

Cold plasma calcination allowed removing ammonia and adsorbed water. The IR bands at 3200 cm^{-1} and 1400 cm^{-1} assigned to N-H stretching vibrations and NH_4 deformation respectively **[47,48]** were completely removed after 15 minutes of cold plasma treatment. The IR band at 1650 cm^{-1} attributed to the bending mode (ν_2) of adsorbed water molecules over the catalyst is also removed after 15 minutes of cold plasma treatment.

3.2.2 Partial ZSM-5 dealumination

H-ZSM-5 zeolites with and without plasma treatment were analyzed by Magic angle spinning ^{27}Al nuclear magnetic resonance. The ^{27}Al-MAS-NMR spectra are presented in Figure 3.

Chemical shifts at 55 and 0 ppm are ascribed to tetracoordinated and hexacoordinated aluminium, respectively **[49,50]**. When calcination was carried out under thermal heating, exclusively tetracoordinated aluminium (FAL) is observed. However, when calcination of ZSM-5 is performed under plasma assistance, both kinds of aluminium, tetracoordinated (FAL) and hexacoordinated (EFAL) were observed. This fact evidences the partial dealumination of ZSM-5 zeolite calcined by cold plasma. In general, after partial dealumination of zeolites, Lewis acidity should be improved.

ZSM-5 template-free zeolite is a very interesting material due to its environmental friendly character. However, it is well-known that template-free zeolites are less stable than zeolites which are synthesized using an organic template. The structure of the template-free ZSM-5 zeolite of this work can more easily collapse during the several physical and chemical treatments needed after its synthesis than that of those synthesized with organic template.

Since more than two decades, the use of cold plasma in the catalysts preparation has been reported **[51]**. In general, zeolites crystallinity can be decreased; their total acidity can be improved and dealumination can be observed after cold plasma treatment. Hu et al. **[46]**

reported a partial dealumination of a MCM-22 material after being irradiated by cold DBD plasma for the elimination of its organic template. In 1989, Maesen et al. **[52]** studied the deammoniation by dry oxygen cold plasma of NH_4-Y zeolite. They found out that faujasite crystallinity is not affected after cold calcination. However, they observed a dealumination of the material. Authors proposed as a possible dealumination mechanism the hydrolysis of framework aluminum (FAL) by protons in Si-OH-Al groupings. Since the temperature of the material is low (cold plasma), low-temperature dealumination cannot be caused through dehydroxylation **[52]**. At high temperature, the dealumination mechanism has been widely proposed **[53,54]**. In this case, successive Al-O bonds are hydrolyzed until dislodgement of the framework Al to a non-framework position to form EFAL species. In the present work, the dealumination mechanism of template-free ZSM-5 during cold oxygen plasma deammoniation could be produced as follows:

i) Highly reactive oxygen species are generated within the low pressure cold glow-like oxygen discharge such as O^-, O^+, metastable O_2, O_2^-, O_3^- and O_3.

ii) The O^- species is the dominant ion in the low pressure (3 mbar) oxygen plasma discharge. This ion is created from dissociative attachments of the O_2 ground state molecule ($^3\Sigma_g^-$) and the metastable O_2 molecule ($a^1\Delta_g$). These species can be consumed by recombination of O^- and O^+ ions. O_3 molecules can be generated by detachment through collision between O^- ions and O_2 metastable molecules. O_2^- species can be as well further created by dissociative attachment of O_3 molecules **[55]**.

iii) The previous highly reactive oxygen species generated in the gas phase could interact with protons from NH_4^+ ions after ammonia desorption to form water molecules. The H_2O molecules could hydrolyze the Al-O bonds displacing thus the FAL species to non-framework positions to give EFAL species.

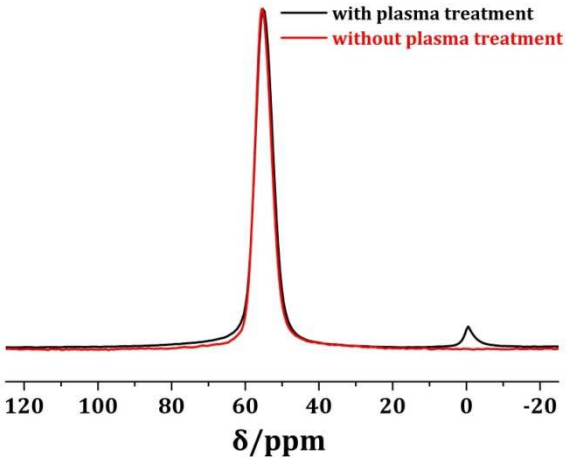

Figure 3: ^{27}Al-MAS-NMR spectra of H-ZSM-5 with and without plasma treatment

3.2.3 In situ FT-IR upon pyridine desorption

Figure 4 shows the amount of pyridine adsorbed onto Lewis (A) and Brønsted (B) acid sites (pyridine denoted as LPy and BPy, respectively), as a function of the evacuation temperature, for both the plasma-activated and reference zeolites. According to references **[56-59]**, the amount of LPy was determined by integrating the IR bands in the region from 1430 to 1470 cm^{-1} (different ones here depending on the evacuation temperature, but same wavenumbers from one sample to the other at each temperature), while the amount of BPy was determined by

integrating the IR band at 1545 cm^{-1} (always centered at the same wavenumber, whatever the evacuation temperature). The molar extinction coefficients to apply the Beer-Lambert law were taken from reference **[56]** (2.22 and 1.67 $cm.\mu mol^{-1}$ for LPy and BPy IR bands respectively). It is worth mentioning that a new type of pyridine species coordinated to Lewis acid sites (LPy2) is observed as a consequence of zeolite dealumination at 1603 and 1446 cm^{-1} **[60-62]**.

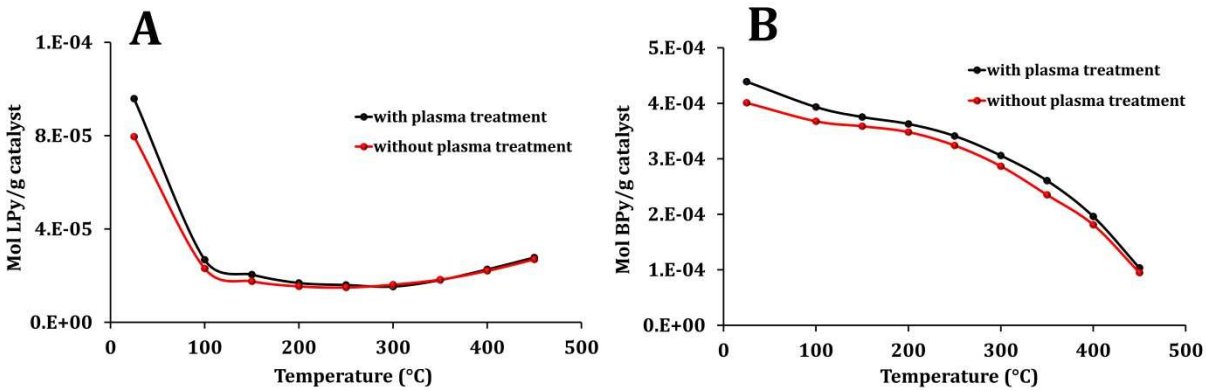

Figure 4: Number of moles of pyridine adsorbed onto Lewis (A) and Brønsted (B) acid sites ~~acidity~~ as a function of evacuation temperature. At 25 °C, this number directly reflects the number of acid sites.

At 25°C, the amount of LPy is higher for the plasma-activated zeolite, reflecting that the latter possesses a higher number of Lewis acid sites compared to the reference zeolite. At higher temperatures, however, the amount of LPy is nearly the same for both zeolites (lower than at 25 °C), indicating that the additional Lewis acid sites possessed by the plasma-activated zeolite are weak (easily leaving pyridine to desorb). Regarding the amount of BPy, it is also higher for the plasma-activated zeolite at 25°C, indicating that the latter zeolite possesses also a higher number of Brønsted acid sites compared to the reference sample. From 25 to 100°C, the gap of BPy amount between the two samples decreases but remains significant. From 100 to 400°C, the gap is even smaller than at 100°C, but it remains quite constant. At 450°C, the amount of BPy is finally the same for both samples. The fact that the amount of BPy is systematically higher for the plasma-activated zeolite up to 400°C can have two possible origins: i) a part of the additional Brønsted acid sites possessed by the plasma-activated zeolite is strong enough to retain pyridine up to 400°C, and ii) a part of the Brønsted acid sites initially present in the zeolite before the plasma treatment became stronger acids due to the plasma treatment, and thus became able to retain pyridine up to 400°C. The second origin is indeed plausible for H-ZSM-5 possessing extra-framework Al species. As reported in **[63]**, the spatial proximities between framework Al (Brønsted acid sites) and extra-framework Al (Lewis acid sites) leads to a synergetic effect that can remarkably enhance the Brønsted acid strength of dealuminated zeolites. In any case, the number of strong Brønsted acid sites (i.e. retaining pyridine up to high temperature) is higher here in the plasma-activated zeolite than in the reference one.

3.3 ZSM-5 catalytic activity in the methanol-to-DME reaction

Catalytic activity of H-ZSM-5 zeolites with and without plasma activation in the methanol-to-DME reaction is presented in Figure 5. The experimental relative error was estimated at 0.5% (error bars are not shown in Figure 5 for clarity improvement).

With its higher number of Lewis and strong Brønsted acid sites, the plasma-activated zeolite leads to a higher methanol conversion (Figure 5A) than the reference zeolite all over the

considered range of reaction temperatures, except at 450°C (same conversion for both samples). Up to 250°C, the selectivity to DME is close to 100% for both samples. Thus, the yield of DME (Figure 5B) is higher for the plasma-activated sample. Above 250°C, by-products start to be formed (alkanes and alkenes and also coke as reflected by Figure 6), making the DME yield of the plasma-activated zeolite decrease to the same level as observed with the reference zeolite.

Indeed, in all mechanisms having been proposed in literature for the condensation of methanol over zeolites, Brønsted acid sites play a key role. In one of the proposed mechanisms, the reaction of methanol requires one Brønsted acid site and one adjacent Lewis basic site to yield two surface species, namely $[CH_3OH_2]^+$ and $[CH_3O]^-$, which upon condensation give DME and water **[64]**. In another mechanism proposed in literature **[64]**, methanol gets protonated on a Brønsted acid site, and the resulting $[CH_3OH_2]^+$ ion gets dehydrated, so leaving a methyl group bonded to the zeolite surface, in other words a methoxy group. The latter then reacts with another methanol molecule to form DME. Blaszkowski et al. proposed that both the latter mechanisms can occur in parallel **[65]**. Actually, Brønsted acidity is what makes zeolites much more active in methanol condensation than the commercially used γ-Al_2O_3 on which Lewis acid sites (weaker) are the active species **[64]**.

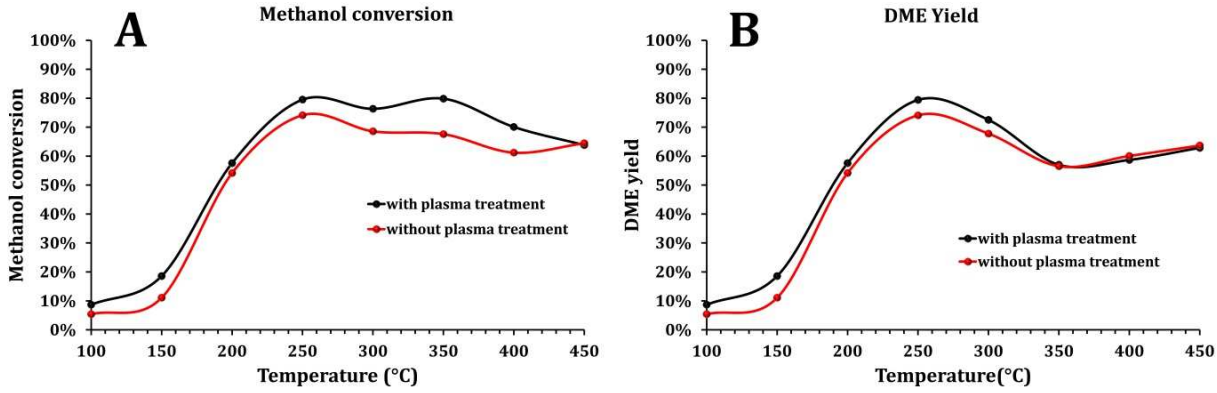

Figure 5: Catalytic activity of H-ZSM-5 zeolites with and without plasma activation

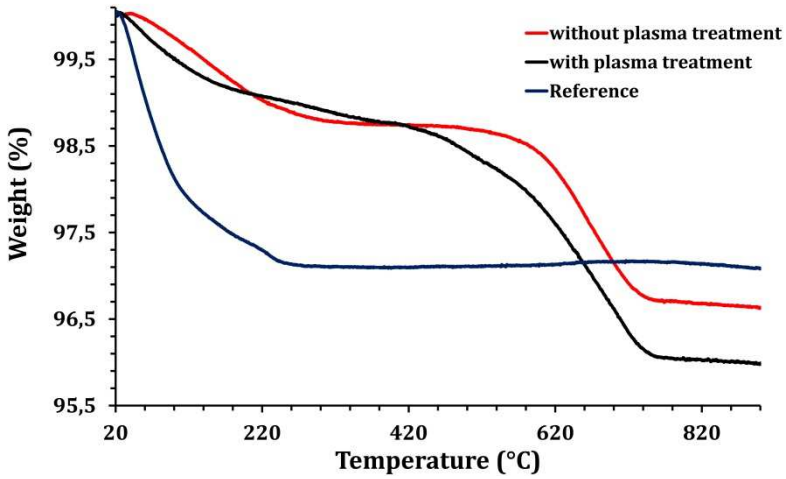

Figure 6: TGA curves of coke burning after catalytic test (compared to a reference before reaction)

In Figure 6, the TGA curves of zeolites with and without plasma activation after catalytic test are shown, as well as a reference (zeolite before reaction). It is possible to observe only water

desorption from the reference sample since it was not used in the methanol-to-DME reaction. Water removal is complete for all samples at 220°C. Coke is decomposed from 420°C . The fact that the plasma-activated zeolite leads to a higher amount of coke deposited after the catalytic test is due to its higher activity above 250°C (see Figure 5).

4 Conclusions

ZSM-5 organic template-free was successfully synthesized by hydrothermal synthesis. NH_4-ZSM-5 zeolite was calcined by thermal heating (without plasma treatment) and by cold plasma (with plasma treatment). In the latter case, only 15 minutes were enough to obtain the H-ZSM-5 form. When plasma was used as zeolite activation method, BET surface area and micropore area were decreased by 5 and 15%, respectively. However, the external surface area was improved by 49% compared to the conventional thermal activation. Pore volume and sizes as well as particle size were not significantly different for both activation methods. When plasma was used as zeolite activation method, a partial zeolite dealumination was verified by XRD, 27Al-MAS-and NMR. As shown through FTIR upon pyridine adsorption-desorption, this partial dealumination increased the number of Lewis acid sites (weak) and the number of Brønsted acid sites (strong) causing an enhancement in the ZSM-5 zeolite catalytic activity in the methanol-to-DME reaction in the whole temperature range under study.

Cold plasma technology is a powerful tool that can be used to activate catalysts (such as zeolites) to improve both Lewis and Brønsted acidity for being used in reactions that require acid catalysts.

Acknowledgements

O.N., J.S. and M.Q. thank F.A.J. for his invitation to work in the LCS Plasma group on this subject. J.S. and F.A.J. acknowledge Marco Daturi for giving J.S. the opportunity to work on this project. Authors finally thank Florian Klipfel and Loïc Le Pluart for TGA analyses.

References

[1] F.S. Ramos, A.M.D. Farias, L.E.P. Borges, J.L. Monteiro, M.A. Fraga, E.F. Sousa-Aguiar, L.G. Appel, Catalysis Today 101 (2005) 39-44.
[2] R.M. Ladera, J.L.G. Fierro, M. Ojeda, S. Rojas, Journal of Catalysis 312 (2014) 195-203.
[3] J. Sun, G. Yang, Y. Yoneyama, N. Tsubaki, ACS Catalysis 4 (2014), 3346-3356.
[4] T.A. Semelsberger, R.L. Borup, H.L. Greene, Journal of Power Sources 156 (2006) 497-511.
[5] L. Dermeche, N. Salhi, S. Hocine, R. Thouvenot, C. Rabia, Journal of Molecular Catalysis A: Chemical 356 (2012) 29-35.
[6] G. Laugel, X. Nitsch, F. Ocampo, B. Louis, Applied Catalysis A: General 402 (2011) 139-145.
[7] A.R. Keshavarz, M. Rezaei, F. Yaripour, Journal of Natural Gas Chemistry 20 (2011) 334-338.
[8] R.M. Ladera, M. Ojeda, J.L.G. Fierro, S. Rojas, Catal. Sci. Technol. 5 (2015) 484-491.
[9] S.S. Akarmazyan, P. Panagiotopoulou, A. Kambolis, C. Papadopoulou, D.I. Kondarides, Applied Catalysis B: Environmental 145 (2014) 136-148.
[10] K.W. Jun, H.S. Lee, H.S. Roh, S.E. Park, Bull. Korean Chem. Soc.24 (2003) 106-108.
[11] H. Schulz, Catalysis Today 154 (2010) 183-194.
[12] E. Catizzone, A. Aloise, M. Migliori, G. Giordano, Microporous and Mesoporous Materials 243 (2017) 102-111.

[13] S. Ivanova, E. Vanhaecke, B. Louis, S. Libs, M.J. Ledoux, S. Rigolet, C. Marichal, C. Pham, F. Luck, C. Pham-Huu, ChemSusChem 1 (2008) 851-857.
[14] H. Fu, W. Song, D.M. Marcus, J.F. Haw, The Journal of Physical Chemistry B 106 (2002) 5648-5652.
[15] W. Alharbi, E.F. Kozhevnikova, I.V. Kozhevnikov, ACS Catalysis 5 (2015) 7186-7193.
[16] J. Schnee, A. Eggermont, E.M. Gaigneaux, ACS Catalysis 7 (2017) 4011-4017.
[17] M. Guisnet, J.P. Gilson, Zeolites for Cleaner Technologies, Catalytic Science Series vol.3, 2002, Imperial College Press.
[18] F. Azzolina-Jury, I. Polaert, L. Estel, L.B. Pierella, Applied Catalysis A: General 453 (2013) 92- 101.
[19] F. Azzolina-Jury, I. Polaert, L.B. Pierella, L. Estel, Catalysis Communications 46 (2014) 6-10.
[20] F. Azzolina-Jury, I. Polaert, L. Estel, L.B. Pierella, Microporous and Mesoporous Materials 198 (2014) 22-28.
[21] F. Azzolina-Jury, I. Polaert, L.B. Pierella, L. Estel, International Journal of Chemical Reactor Engineering 13 (2015) 169-175.
[22] F. Azzolina-Jury, F. Thiabult-Starzyk, Current Microwave Chemistry, 3 (2016) 102-113.
[23] F. Azzolina-Jury, F. Thibault-Starzyk, Topics in Catalysis 60 (2017) 1709-1721.
[24] F. Azzolina-Jury, D. Bento, C. Henriques, F. Thibault-Starzyk, Journal of CO_2 Utilization 22 (2017) 97-109.
[25] N.J. Abreu, H. Valdés, C.A. Zaror, F. Azzolina-Jury, M.F. Meléndrez, Microporous and Mesoporous Materials 274 (2019) 138-148.
[26] M.D. González, Y. Cesteros, P. Salagre, Microporous and Mesoporous Materials 144 (2011) 162-170.
[27] A.K. Ghosh, R.A. Kydd, Zeolites 10 (1990) 766-771.
[28] Z. Qin, L. Lakiss, J.-P. Gilson, K. Thomas, J.-M. Goupil, C. Fernandez, V. Valtchev, Chemistry of Materials 25 (2013) 2759-2766.
[29] N.S. Nesterenko, F. Thibault-Starzyk, V. Montouillout, V.V. Yuschenko, C. Fernandez, J.-P. Gilson, F. Fajula, I.I. Ivanova, Microporous and Mesoporous Materials 71 (2004) 157-166.
[30] C. Fernandez, I. Stan, J.-P. Gilson, K. Thomas, A. Vicente, A. Bonilla, J. Perez-Ramirez, Chem. Eur. J. 16 (2010) 6224-6233.
[31] F. Thibault-Starzyk, I. Stan, S. Abelló, A. Bonilla, K. Thomas, C. Fernandez, J.-P. Gilson, J. Pérez-Ramírez, Journal of Catalysis 264 (2009) 11-14.
[32] C.-j. Liu, G.P. Vissokov, B.W.-L. Jang, Catalysis Today 72 (2002) 173-184.
[33] Z. Wang, Y. Zhang, E.C. Neyts, X. Cao, X. Zhang, B.W.-L. Jang, C.-j. Liu, ACS Catalysis 8 (2018) 2093-2110.
[34] T.L.M. Maesen, H.W. Kouwenhoven, H. van Bekkum, B. Sulikowsk, J. Klinowski, Journal of the Chemical Society, Faraday Transactions, 86 (1990) 3967-3970.
[35] M. El-Roz, L. Lakiss, V. Valtchev, S. Mintova, F. Thibault-Starzyk, Microporous and Mesoporous Materials 158 (2012) 148-154.
[36] M. Hu, B. Zhao, D.-Y. Zhao, M.-T. Yuan, H. Chen, Q.-Q. Hao, M. Sun, L. Xu, X. Ma, RSC Advances, 8 (2018) 15372-15379.
[37] F. Azzolina-Jury, Journal of Industrial and Engineering Chemistry, 71 (2019) 410-424
[38] R. Debek, D. Wierzbicki, M. Motak, M.E. Galvez, P. Da Costa, F. Azzolina-Jury, Plasma Science and Technology 21 (2019) 045503
[39] C.-j. Liu, K. Yu, Y.-p. Zhang, X. Zhua, F. Hea, B. Eliasson, Applied Catalysis B: Environmental 47 (2004) 95-100.
[40] Y.-P. Zhang, P.-S. Ma, X. Zhu, C.-J. Liu, Y. Shen, Catalysis Communications 5 (2004) 35-39.
[41] V.P. Shiralkar, A. Clearfield, Zeolites 9 (1989) 363-370.
[42] K.P. Dey, S. Ghosh, M.K. Naskar, Ceramics International 39 (2013) 2153-2157.
[43] Hartati, A. Akustia, I. Permana, D. Prasetyoko, AIP Conference Proceedings 1718, 060002 (2016); doi: 10.1063/1.4943324
[44] L. Zhang, S. Liu, S. Xie, L. Xu, Microporous and Mesoporous Materials 147 (2012) 117-126.
[45] Y. Cheng, L.-J. Wang, J.-S. Li, Y.-C. Yang, X.-Y. Sun, Materials Letters 59 (2005) 3427-3430.

[46] M. Hu, B. Zhao, D-Y. Zhao, M-T. Yuan, H. Chen, Q-Q. Hao, M. Sun, L. Xu, X. Ma, RSC Adv. 8 (2018), 15372
[47] T.L.M. Maesen, B. Sulikowski, H. Van Bekkum, H.W. Kouwenhoven, J. Klinowski, Applied Catalysis, 48 (1989) 373-383.
[48] J.-P. Gilson, C. Fernandez, F. Thibault-Starzyk, Journal of Molecular Catalysis A: Chemical 305 (2009) 54-59.
[49] L. Rodriguez-Gonzalez, F. Hermes, M. Bertmer, E. Rodriguez-Castellon, A. Jimenez-Lopez, U. Simon, Applied Catalysis A: General 328 (2007) 174-182.
[50] C.S. Triantafillidis, A.G. Vlessidis, L. Nalbandian, N.P. Evmiridis, Microporous and Mesoporous Materials 47 (2001) 369-388.

[51] M.B. Kizling, S.G. Jaras, Applied Catalysis A: General 147 (1996) 1-21
[52] T.L.M. Maesen, B. Sulikowski, H. Van Bekkum, H.W. Kouwenhoven, J. Klinowski, Applied Catalysis, 48 (1989) 373-383
[53] M-C. Silaghi, C. Chizallet, J. Sauer, P. Raybaud, Journal of Catalysis 339 (2016) 242-255
[54] H.G. Karge, J. Weitkamp, "Post-Synthesis Modification I", Vol.3 (2002) Springer-Verlag Berlin Heidelberg
[55] J.T. Gudmundsson, G. Kouznetsov, K.K. Patel, M.A. Lieberman, Journal of Physics D: Applied Physics 34 (2001) 1100-1109
[56] C.A. Emeis, Journal of Catalysis, 141 (1993) 347-354.
[57] S. Lai, D. Meng, W. Zhan, Y. Guo, Y. Guo, Z. Zhang, G. Lu, RSC Advances, 5 (2015) 90235-90244.
[58] D. Hartanto, L. Yuan, S. Sari, D. Sugiarso, I. Murwani, T. Ersam, D. Prasetyoko, H. Nur, Jurnal Teknologi 78 (2016) 223-228.
[59] N. Brodu, M.-H. Manero, C. Andriantsiferana, J.-S. Pic, H. Valdés, Chemical Engineering Journal, 231 (2013) 281-286.
[60] J.P. Marques, I. Gener, P. Ayrault, J.C. Bordado, J.M. Lopes, F. Ramoa Ribeiro, M. Guisnet, Microporous and Mesoporous Materials 60 (2003) 251-262.
[61] B.H. Chiche, F. Fajula, E. Garrone, Journal of Catalysis 146 (1994) 460-467.
[62] K. Sang Yoo, S. Gopal, P.G. Smirniotis, Industrial & Engineering Chemistry Research 44 (2005) 4562-4568.
[63] Z. Yu, S. Li, Q. Wang, A. Zheng, X. Jun, L. Chen, F. Deng, The Journal of Physical Chemistry C, 115 (2011) 22320-22327.
[64] H. Ajami, A. Shariati, Journal Energy Sources, Part A: Recovery, Utilization, and Environmental Effects 38 (2016) 2845-2853.
[65] S. Jiang, J.-S. Hwang, T.-H. Jin, T. Cai, W. Cho, Y.-S. Baek, S.-E. Park, Bulletin- Korean Chemical Society 25 (2004) 185-189.

Plasma activation

ZSM-5 organic template-free synthesis

Brønsted and Lewis acidity enhancement

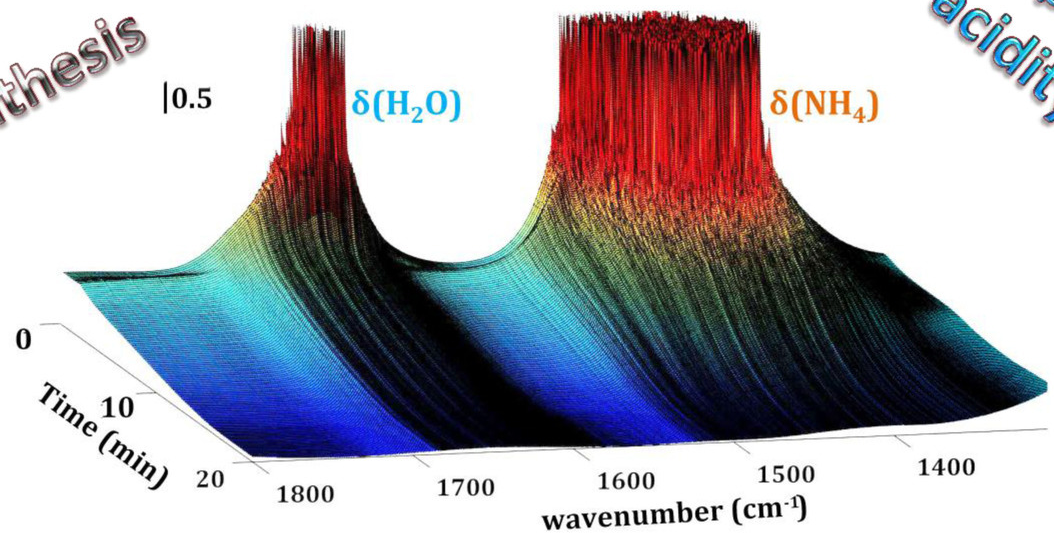

Methanol-to-DME catalytic activity improvement